Untargeted gas chromatography–mass spectrometry-based metabolomics analysis of kidney and liver tissue from the Lewis Polycystic Kidney rat

Hayley Abbiss, Garth L. Maker, Joel P.A. Gummer, Catherine Rawlinson, Gabrielle C. Musk, Patricia A. Fleming, Jacqueline K. Phillips, Mary C. Boyce, Robert D. Trengove

PII: S1570-0232(18)31803-8
DOI: https://doi.org/10.1016/j.jchromb.2019.04.021
Reference: CHROMB 21601

To appear in: *Journal of Chromatography B*

Received date: 5 December 2018
Revised date: 19 March 2019
Accepted date: 11 April 2019

Please cite this article as: H. Abbiss, G.L. Maker, J.P.A. Gummer, et al., Untargeted gas chromatography–mass spectrometry-based metabolomics analysis of kidney and liver tissue from the Lewis Polycystic Kidney rat, Journal of Chromatography B, https://doi.org/10.1016/j.jchromb.2019.04.021

Untargeted gas chromatography-mass spectrometry-based metabolomics analysis of kidney and liver tissue from the Lewis Polycystic Kidney rat

Hayley Abbiss[1,2*], Garth L. Maker[1,2], Joel P.A. Gummer[1,2,3], Catherine Rawlinson[2,3], Gabrielle C. Musk[4], Patricia A. Fleming[1], Jacqueline K. Phillips[5], Mary C. Boyce[6], Robert D. Trengove[2,3]

1 School of Veterinary and Life Sciences, Murdoch University, 90 South Street, Murdoch WA 6150, Australia

2 Separation Science and Metabolomics Laboratory, Murdoch University, 90 South Street, Murdoch WA 6150, Australia

3 Metabolomics Australia, Western Australia Node, Murdoch University, Murdoch University, 90 South Street, Murdoch WA 6150, Australia

4 Animal Care Services, The University of Western Australia, 35 Stirling Highway, Crawley, WA, 6009, Australia

5 Department of Biomedical Science, Faculty of Medicine and Health Sciences, Macquarie University, Sydney, NSW, Australia

6 School of Science, Edith Cowan University, 270 Joondalup Drive, Joondalup, WA 6027, Australia

[*]Address correspondence to: Dr Hayley Abbiss, Separation Science and Metabolomics Laboratory, Building 223, Murdoch University, 90 South Street, Murdoch WA 6150, Australia. Tel: +61 8 9360 6592. Email: H.Abbiss@murdoch.edu.au

Abstract

Polycystic kidney disease (PKD) encompasses a spectrum of inherited disorders that lead to end-stage renal disease (ESRD). There is no cure for PKD and current treatment options are limited to renal replacement therapy and transplantation. A better understanding of the pathobiology of PKD is needed for the development of new, less invasive treatments. The Lewis Polycystic Kidney (LPK) rat phenotype has been characterized and classified as a model of nephronophthisis (NPHP9, caused by mutation of the Nek8 gene) for which polycystic kidneys are one of the main pathologic features. The aim of this study was to use a GC-MS-based untargeted metabolomics approach to determine key biochemical changes in kidney and liver tissue of the LPK rat. Tissues from 16-week old LPK (n = 10) and Lewis age- and sex-matched control animals (n = 11) were used. Principal component analysis (PCA) distinguished signal corrected metabolite profiles from Lewis and LPK rats for kidney (PC-1 77%) and liver (PC-1 46%) tissue. There were marked differences in the metabolite profiles of the kidney tissues with 122 deconvoluted features significantly different between the LPK and Lewis strains. The metabolite profiles were less marked between strains for liver samples with 30 features significantly different. Five biochemical pathways showed three or more significantly altered metabolites: transcription/translation, arginine and proline metabolism, alpha-linolenic and linoleic acid metabolism, the citric acid cycle, and the urea cycle. The results of this study validate and complement the current literature and are consistent with the understood pathobiology of PKD.

Keywords

Gas chromatography; mass spectrometry; metabolomics; nephronophthisis; polycystic kidney disease

1. Introduction

Inherited kidney diseases contribute considerably to the number of patients suffering from chronic kidney disease (CKD) and requiring renal replacement therapy. The most common inherited kidney disease is autosomal dominant polycystic kidney disease (ADPKD), which presents in adulthood and is caused by mutations in the Pkd1 or Pkd2 genes [1]. ADPKD has an estimated incidence of 1:400-1,000 [2]. Polycystic kidneys are also the main pathologic feature of autosomal recessive (AR) PKD [2]. ARPKD, caused by mutations in the Pkhd1 gene and typically presenting in childhood, is less common with an incidence of approximately 1:20,000 [2, 3]. The nephronophthisis (NPHP) group of ciliopathies, with a recessive pattern of inheritance and over 20 associated genes [4, 5], presents in childhood and has an incidence of 1:50,000-900,000. Simms *et al*. [6] suggest that this figure is likely to be an underrepresentation due to the late diagnosis of NPHP in adults with advanced CKD.

Ranging in severity [7] and encoded by different genes (e.g. Pkd1 and Pkd2 encode polycystin-1 and -2, while Pkhd1 encodes fibrocystin/polyductin), each form of PKD produces a cystic kidney phenotype for which extra-renal and mechanistic similarities have been described [8-10]. Examining the mechanism(s) of cyst formation, proliferation and expansion will be beneficial to an understanding of all of the described cystic kidney phenotypes. Although there are treatments which target the biochemical pathways associated with these events advancing to clinical trials [9], current management strategies involve mediating complications associated with renal failure, such as increased blood pressure and cardiovascular disease [2], and managing pain [11]. Currently, the only treatments available for PKDs are renal replacement therapy and transplantation.

There are numerous reports of the use of biofluids for metabolomics and proteomics analyses of CKD [12-18]. Biofluids are easily obtained, collection is non-invasive, and urine (in particular) has been of interest for studies of kidney disease and the detection of

biomarkers. Due to this interest, few metabolomics studies of CKD, or indeed PKD, have focused on the diseased organs. It has been suggested that PKD pathobiology may be driven by metabolic perturbations [19] and recently, metabolomics-based approaches to the study of PKD have emerged [12, 14, 15, 18, 20]. While metabolomics studies investigating biofluids of the mouse [14, 20] and rat [12, 15] polycystic kidney phenotype have been reported, only one other study investigating PKD tissue has been reported [20], although tissue-based metabolomics investigations of other models of chronic kidney disease have been carried out [21, 22].

In the present study, kidney tissue samples for a genetically- and phenotypically-characterised [23-25] NPHP (NPHP9) PKD model, arising as a spontaneous mutation in a Lewis rat strain, were investigated to determine biochemical changes related to the underlying pathobiology. We also investigated liver tissue because, despite gross liver cyst formation not being a pathological feature of the Lewis polycystic kidney (LPK) rat [24], the liver has been implicated in the NPHP phenotype [6, 26], as well as in other forms of PKD [10, 27]. In addition to elucidating biochemical changes in the polycystic kidney phenotype, we determine whether there was any consistency between the significant metabolites for the PKD model with biomarkers for PKD proposed in the literature.

2. Materials and Methods

2.1 Animals

All experiments were conducted with approval from the relevant animal ethics committee in accordance with the Australian Code of Practice for the Care and Use of Animals for Scientific Purposes (8th Edition, 2013) as endorsed by the National Health and Medical Research Council of Australia. Ten 16-week old LPK rats (7 male; 3 female) and 11 Lewis (LEW/CrlBR; 7 male; 4 female) control animals (Animal Resources Centre; Canning Vale,

WA, Australia) were used. Animals were studied at age 16 weeks based on our previous work demonstrating this as a time point when renal disease is established and other systemic markers such as urea and creatinine are significantly elevated but before the animals have progressed to end stage renal failure [24]. Animals were housed two or three per cage in a 12h:12h light:dark cycle with non-regulated environmental temperature and humidity. Animals had access to standard laboratory chow and tap water *ad libitum*.

2.2 Chemicals and reagents

Chemicals and reagents were purchased from Sigma-Aldrich (Castle Hill, NSW, Australia) in the highest purity available. LC-MS grade methanol, water and laboratory consumables were purchased from Thermo Fisher Scientific (Scoresby, VIC, Australia).

2.3 Sample collection

Animals were anesthetized using isoflurane (ISO; Veterinary Companies of Australia, Blacktown, NSW, Australia) vapour (induction: 4% ISO in 6 L min^{-1} of 100% O_2; maintenance: 2% ISO in 2 L min^{-1} of 100% O_2) and euthanized by exsanguination. A kidney and the liver were harvested immediately, washed with physiological saline solution, packaged separately in plastic zip-lock bags and frozen on dry ice. Organs were stored at -80°C until further use.

2.4 Metabolite extraction

Organs were transferred frozen to plastic specimen jars, weighed (frozen wet weight) and then freeze-dried whole for 3-5 days using a FreeZone 2.5 Plus freeze-dryer (Labconco corp., Kansas City, MO, USA). Once dry, the organ dry weight was recorded. After the removal of any visible adipose tissue (fat pad), the organs were ground using a mortar and pestle. Approximately 5 mg of tissue was weighed into a Precellys soft tissue homogenization tube

(2 mL; beads removed; Bertin Instruments, Montigny-le-Bretonneux, France) and the weight recorded (±0.00001 g). Ceramic beads were returned to the tubes after weighing the sample.

Samples were milled using a Precellys homogenizer (Bertin Instruments, Montigny-le-Bretonneux, France) for 20 s at 6500 rpm, returned to dry ice and then milled a second time for 20 s at 6500 rpm. At this point, samples were either 'paste-like' or a very fine powder. LC-MS grade methanol (500 µL) was added to the milled sample which was then returned to the homogenizer for a further two runs of 20 s at 6500 rpm. Samples were agitated (Eppendorf Thermomixer Comfort; Eppendorf South Pacific Pty Ltd, North Ryde, NSW, Australia) at 1200 rpm for 5 min. Samples were then centrifuged (Eppendorf 5415R centrifuge; Eppendorf South Pacific Pty Ltd, North Ryde, NSW, Australia) at 16100 × *g* at 4°C for 5 min. The supernatant was transferred to a fresh 2 mL tube and stored on dry ice. The methanol extraction procedure was repeated on the tissue sample and supernatants combined. LC-MS grade water (300 µL) containing the uniformly labelled internal standard (IS; $^{13}C_6$-sorbitol; 3.25 µg.mL^{-1}) to assess extraction, derivatisation and instrument performance was then added to the tissue sample and the extraction procedure was repeated for a third time. Samples were maintained on dry ice at all times possible throughout the extraction procedure. After an overnight 'freeze-out' at -80°C, the combined extract was centrifuged (16,100 × *g* at 4°C for 5 min) and the resulting supernatant was transferred to a clean tube. The methanol was evaporated from the extract in an Eppendorf Concentrator Plus rotary vacuum concentrator. LC-MS grade water (400 µL) was added to the extracts, which were then frozen on dry ice before freeze-drying overnight. Dried extracts were stored at -80°C until derivatization and analysis.

2.5 Metabolite derivatization

Dry metabolites were treated with 40 µL methoxyamine-HCl (20 mg.mL^{-1} in pyridine) and mixed for 90 min at 1,200 rpm and 30°C in the Thermomixer. Following methoximation,

metabolites were treated with 80 µL MSTFA and mixed for 30 min at 300 rpm and 37°C. The derivatized mixture was transferred to a GC vial containing 10 µL of an alkane mix in hexane (C_{10}, C_{12}, C_{15}, C_{19}, C_{22}, C_{28}; 0.156 mg.mL^{-1}; C_{32}, C_{36}; 0.313 mg.mL^{-1}).

2.6 Instrumental analysis

A Shimadzu GC 2010Plus coupled to a Shimadzu QP2010Ultra MS system with an AOC-20i autosampler and injector unit was used (Shimadzu Scientific Instruments, Rydalmere, NSW, Australia). The column used was an Agilent Factor Four fused silica capillary column VF-5ms (30 m × ID = 0.25 mm × DF = 0.25 µm + 10 m EZ-Guard; Agilent Technologies, Palo Alto, CA, USA). The derivatized sample (1 µL) was injected in splitless mode into the inlet at a temperature of 230°C. The initial column temperature was set to 70°C. A temperature ramp of 1°C.min^{-1} for 5 min followed by a temperature ramp of 5.63°C.min^{-1} to a final temperature of 330°C with a hold time of 10 min was used. The carrier gas used was helium and the head pressure was set such that mannitol (6-trimethylsilyl derivative) would elute at 30.6 min. The transfer line was set to 330°C and the ion source was set to 200°C. Ionization was achieved with a 70 eV electron beam and the mass analyzer was operated in full scan mode over the range *m/z* 45-600 with a scan rate of 10 spectral scans per second.

2.7 Data processing and analysis

Full scan data was processed using AnalyzerPro™ v2.7 (SpectralWorks, Runcorn, Cheshire, UK). Peak detection parameter settings are tabulated in Supporting Information Table SI1. A script written in Ruby programming language was used for alignment of common chromatographic peaks as previously described [28, 29]. For kidney tissue samples, metabolites which occurred in at least 17 of 21 replicates (> 80%) or all replicates of one strain and none of the other were considered. For liver tissue samples, metabolites which

occurred in at least 15 of 19 replicates (> 78%) were considered. For kidney and liver tissue, missing values were replaced with the lowest recorded peak area for the strain. In the first instance, peak area was scaled to the sample weight (mg dry weight) and transformed ($x=\log_{10}[x+1]$) and in the second instance to the sample weight and internal standard, and $\log_{10}$-transformed (as above; see result section 5.3.2). Data matrices are provided in Supplementary files SI2 and SI3. Principal component analyses (PCA) were conducted using The Unscrambler X v10.1 (CAMO, Oslo, Norway). Data were mean centered, cross validated using the non-linear iterative partial least squares (NIPALS) approach and 7 components were generated.

Log-scaled peak area of the IS for kidney and liver experiments was assessed for strain effects using the Mann-Whitney U-test and correlation between the IS and the TIC; and IS and the sum of peak areas in the final peak table was assessed using Spearman's Rho (SPSS v22.0, IBM Corp., Armonk, NY, USA) All other data were assessed for statistical significance using the MATLAB scripting language (v2017b, MathWorks, Natick, MA, USA). Independent t-tests assuming unequal variance were conducted on a per-compound basis to determine the effect of strain on metabolites and the Benjamini-Hochberg [30] false discovery rate correction was used. Uncorrected (p-values) and corrected (q-values) are reported. A $p < 0.05$ threshold for statistical significance and 95% confidence interval were employed for Mann-Whitney and t-tests and values were expressed as means ± 1 SD throughout.

2.8 Metabolite identification

All unique features were assigned an identification number as a prefix. Significant deconvoluted features were named according to their ID number and metabolite identification or, where identification was not possible, ID number, compound class or 'unknown', retention index and base peak. Metabolite identifications were made by comparing mass

spectra and retention index with a user-generated library of authentic analytical standards (match >80%; Metabolomics Australia, Murdoch University). Putative identifications were made using the National Institute of Standards and Technology (NIST) 2011 MS Search v2.0 library (Gaithersburg, MD, USA) with confidence scores >70% and probability scores >20% as previously described [28]. Information pertaining to the identification of features including scores representing the confidence of the identifications can be found in the online supplementary material (Tables SI5 and SI7). The Human Metabolome Database v3.6 [31-33] was used to assign compound classes (sub-classes) and biochemical pathways. Pathways were drawn using VANTED v2.2.1. [34].

3. Results

3.1 Gross features of the LPK kidney and liver tissues

At 16 weeks of age, LPK rats were only two-thirds the body mass of age-matched Lewis control rats ($p = 0.003$; Table 1). At the time organs were harvested, very little normal kidney tissue was evident macroscopically (Figure 1), and the LPK kidneys were six times heavier than those from Lewis controls ($p < 0.001$; Table 1). By contrast, livers from LPK rats were around half the weight of the Lewis control rats ($p < 0.001$; Table 1); this was not solely due to the significantly lower body mass of the animals, as the wet and dry livers also weighed significantly less when calculated as %BW compared to Lewis controls (Table 1). These findings are in agreement with previous work [24].

3.2 Reproducibility of metabolomics analyses

The added IS, for the analysis of kidney metabolites, was examined to determine whether the measured signal represented the response of all measured features. The deconvoluted peak area of the IS correlated significantly to the sum of the peak area (Spearman's Rho; $r = 0.719$; $p < 0.001$) and the TIC (Spearman's Rho; $r = 0.979$; $p < 0.001$); considered acceptable

values for the normalization of metabolomics data. However, as the IS representative only of a single chemical class, it was further interrogated. The calculated relative standard deviation (RSD) of the IS was 62%, higher than the 30% which deemed appropriate for large-scale GC-MS analyses utilizing silylation for the derivatisation of polar metabolites [35]. The mean area of the IS in the LPK samples was also significantly greater than the Lewis control ($p < 0.001$; 3.5-fold); reproducibility of the internal standard for LPK samples was 19%, while for the Lewis control it was 27%. As such, to avoid the bias of using an imperfect IS-correction, the data were subsequently interrogated both with and without signal correction, and only those metabolites found significant between strains using the two approaches and with the same fold change direction reported. Metabolites which were significant using only one approach (uncorrected or corrected) or showed different fold change direction for uncorrected and corrected data were not reported.

As samples were randomised prior to analysis, the significant difference observed for the internal standard was not due to changing instrument response as a result of a batched analysis. To further confirm this, the average response of the added alkane standards was also interrogated, and a 25% relative standard deviation determined. Interestingly, this observation does appear to be specifically related to LPK kidney tissue since the same trend was not seen in the liver analyses (described below), and the Lewis healthy kidney tissue showed a similar IS response to the LPK and Lewis liver tissues (RSD = 25%).

For the liver data, two outlier samples were identified, which had decreased maximum intensity (mean 4.09-fold decrease), TIC intensity (mean 1.77-fold decrease), and internal standard response (mean 2.93-fold decrease). Since the *n*-alkane RSD was in the range of 16–22% with outliers and 17–23% without outliers, an extraction or derivatization inefficiency was likely the cause. The IS RSD for the liver analysis was 28% before and 19% after removal of these two described outliers. There was no significant difference in IS

measurement (Mann-Whitney U-test $p = 0.051$) for liver tissues; however, the internal standard was only significantly correlated to the TIC (Spearman's Rho; $r = 0.788$; $p < 0.001$) and not to the sum of peak areas used in further analyses (Spearman's Rho; $r = 0.223$; $p = 0.359$). For consistency, the liver data was treated as described for the kidney data.

3.3 The majority of reproducibly detected metabolites in the LPK rat kidney were significantly different from the Lewis control

Approximately twice the number of deconvoluted features were detected in LPK kidneys compared with the Lewis controls (Table 2). Seventy-three features were unique to the LPK rat kidney, and 12 to the Lewis. 146 deconvoluted features were common to both strains and detected in >80% of replicates (231 features total; Table 2). The composition of metabolites was significantly different between LPK and Lewis kidneys (PCA for uncorrected data: PC-1, 99%, Figure 2A; internal standard-corrected data: PC-1, 77%, Figure 2C). In the PCA loadings plots (Figure 2B and 2D), compound 646 (succinic acid 2TMS) appears to have the most influence on the separation of the LPK from the Lewis kidney samples. One hundred and twenty-two features were significantly different between strains. Several amino acids were decreased in LPK kidney samples (0.1–0.5-fold changes; $p < 0.046$; Table SI4). One amino acid increased (tyrosine, ≥6.7-fold change; $p < 0.001$), and two amino acids (1-methylhistidine, tryptophan) were present in the LPK kidney samples but not detected in Lewis samples. Four carboxylic acids were significantly decreased in the LPK kidney samples (0.1–0.7-fold changes; $p \leq 0.038$), including two (succinic and itaconic [methylene succinic] acids) which were not detected. Two carboxylic acids (malic and citric acids) were significantly increased in the LPK kidney samples (≥ 1.6-fold change; $p \leq 0.016$) and hippuric acid was only detected in LPK samples. Several fatty acids were significantly decreased (≤0.7-fold change; $p \leq 0.031$). Significant increases in monosaccharides were noted for LPK kidney samples, including several which were not detected in the Lewis

samples. Urea was significantly increased in the LPK kidney samples (≥2.3-fold change; $p \leq 0.012$). There also appears to be variation in the metabolite profiles of males and females for LPK samples (Figure 2A and C). We note here that three metabolites found to be significant in the literature were also found in this study but fell below our reporting criteria (present in 100% of one strain or 80% of all study samples; significant between strains with the same fold change direction for IS- and non-IS-corrected data).

We were able to putatively identify 47 unique metabolites that were significantly different between PKD and Lewis kidney samples (Tables 2 and 3). Five biochemical pathways were determined to have three or more significant metabolites: 1. transcription/translation, 2. arginine and proline metabolism, 3. alpha-linolenic and linoleic acid metabolism, 4. the citric acid cycle and 5. the urea cycle. Many of the metabolites identified are common to the abovementioned pathways. For example, aspartic acid plays a role in arginine and proline metabolism, transcription and translation, and the urea cycle. Similarly, fumaric acid has roles in arginine and proline metabolism, the citric acid cycle and the urea cycle.

3.4 Few metabolites of the LPK rat liver were significantly different from the Lewis control.

There was little difference in the number of features detected in the LPK and Lewis liver control samples (Table 2). 167 features were deconvoluted in > 78% of the liver tissue replicates (15 of 19). No features were unique to liver samples of either strain of rat, although 30 features were found to be significantly different between strains ($p < 0.05$; Table 2). PCA distinguished LPK from Lewis liver samples in male rats (uncorrected: PC-1 28%, Figure 3A; internal standard-corrected: PC-1 46%, Figure 3C), but there was no distinction between disease states for females (Figure 3). The untransformed values (Figure 3A) were not influenced by a single outlier, whereas the transformed values were. Among other significant differences (Table SI5), there was a ~2-fold increase in four amino acids ($p \leq 0.043$) and two

fatty acids ($p \leq 0.030$) in the LPK rat. Urea was significantly increased in the LPK liver (~1.5-fold change; $p \leq 0.036$). Fourteen unique metabolites were putatively identified in the liver tissue (Tables 2 and 4).

4. Discussion

The key finding of this study is the identification of numerous metabolites in the kidney and liver organ tissues that were significantly different in abundance between normal and PKD samples. The significantly different metabolites correspond to biochemical pathways associated with disease pathobiology (particularly altered energy metabolism) that are similarly identified in the reported literature [20, 24]. This study therefore supports the current hypotheses that PKD exhibits characteristics of enhanced metabolism [36] and malignant processes [20], and that the pathways associated with cell proliferation and organ tissue growth may be appropriate targets for intervention.

We found marked differences in the metabolic profile of LPK rat kidneys, which matched the gross anatomical changes evident at 16 weeks of age. Most notable were changes in five biochemical pathways: 1. transcription/translation, 2. arginine and proline metabolism, 3. alpha-linolenic and linoleic acid metabolism, 4. the citric acid cycle and 5. the urea cycle. The five metabolic pathways identified as different between LPK and Lewis rat strains are relevant to PKD pathobiology. Notably, there were fewer anatomical changes in LPK liver tissue samples, although we nevertheless noted substantial changes in the metabolite profiles of these tissue samples.

4.1 Kidney tissue changes

4.1.1 Transcription and translation

Here we have shown five significantly different amino acids that are related to transcription and translation (being aspartic acid, cysteine and proline which were significantly decreased in the LPK kidney tissue samples, and tryptophan and tyrosine which were significantly increased). Notably, proline, tryptophan and tyrosine have been shown as important in other metabolomic studies of PKD [14, 18] and CKD [13]. Differences in several amino acids in the PKD phenotype may be linked to reported differences in protein metabolism. Kistler *et al*. [16] used a proteomics approach to study urinary protein in ADPKD patients with preserved renal function. Their findings included differences in extracellular matrix collagen fragments and uromodulin [16]. Moreno *et al*. [17] also used a proteomics approach and were able to distinguish untreated ADPKD patients from treated (roscovitine) and healthy subjects. Additionally, Gronwald *et al*. [18] determined that there were several significantly different urinary proteins between human ADPKD compared with healthy controls using a NMR spectroscopy metabolite fingerprinting approach.

4.1.2 Arginine and proline metabolism and the urea cycle

Aspartic acid, fumaric acid and proline were decreased in LPK kidney tissue and urea was increased, which may indicate changes in arginine and proline metabolism. Within mammals, citrulline (from which arginine is synthesized) is largely formed by the catabolism of amino acids (including glutamate and glutamine) within the small intestine; the majority of which is subsequently metabolised in the kidneys for the biosynthesis of arginine, following extraction from circulation by the proximal tubules [37-39]. Impairment of kidney function therefore impacts arginine and proline metabolism. While proline was decreased in diseased animals within this study; it is not possible to distinguish whether this decrease represents

biochemical change or a result of the deterioration in filtering capacity of the kidneys, since it is known that 16-week old LPK animals experience significantly decreased renal function [24], and proline has been identified as a uremic solute [13]. Since the removal of nitrogenous waste is a key function of the kidney and we have shown changes in aspartic and fumaric acids and urea, it was expected that the urea cycle would be perturbed. Decreased aspartic and fumaric acids may result in the accumulation of arginine and citrulline however we have not observed this. Since neither metabolite was detected, future research should aim to target these metabolites in this model.

4.1.3 Alpha-linolenic and linoleic acid metabolism

Alpha-linolenic and linoleic acid metabolism is related to cell signaling processes [37, 38]. During the expansion of encapsulated cysts, signaling pathways become activated or dysfunctional, resulting in increased cyst growth [8] and as such, changes in metabolites (arachidonic acid, docosahexaenoic acid and eicosatrienoic acid) in this pathway would be consistent with PKD pathogenesis.

4.1.4 The citric acid cycle

The citric acid cycle (Figure 5.4) has been proposed as a key pathway implicated in PKD pathogenesis. Hwang *et al*. [20] concluded for both mouse (kidney tissue, serum and urine) and human PKD (kidney tissue) that PKD cells are dependent on glutamine and direct the TCA cycle toward the production of the oncometabolite 2-hydroxyglutaric acid. We found that 2-hydroxyglutaric acid was indeed increased in LPK kidney samples; however, it was only detected in 15 of 21 samples which was below our processing criteria for reproducible detection (i.e. present in ≥80% of sample set). Similarly, 2-oxoglutaric acid was increased in LPK kidney samples and glutamic acid was decreased but neither met the minimum reporting criteria. Interestingly, between the present study and that of Hwang *et al*. [20] two differences

identified were that 1) glutamine was not detected in this study and 2) malic acid was significantly increased in our LPK samples (Figure 4). Hwang et al. used a more sensitive method for the detection of glutamine which may explain the first difference. Mouse model (cpk) and human tissues were used in their study which may explain the second difference. Additionally, our samples were collected at a late stage of disease whereas those used by Hwang et al were from early stages (cpk = 14 days old; human = < 1 year old). Many of the metabolites reported in the present study have previously been reported as uremic retention solutes in human plasma of CKD patients [13] and Cy/+ rat plasma [12]. We observed many synonymous results including increased citric acid, erythronic acid, glutamic acid, hippuric acid, 4-hydroxyhippuric acid, pseudouridine, urea and uric acid. An increase in tryptophan in PKD kidney tissue was found in this study however, Boelaert et al., [13] found decreased tryptophan within the plasma of CKD patients indicating that this metabolite may not be a uremic retention solute. Indeed, it has been shown previously that decreased blood tryptophan is associated with renal disease [40, 41].

All of the above-mentioned metabolites, with the exception of erythronic acid, 4-hydroxyhippuric acid and proline distinguish the urine of PKD rodent models from healthy controls [14, 15]. Further, ethanolamine, fucose, fumaric acid, hexadecanoic acid, 2-hydroxyglutaric acid, malic acid, 2-oxoglutaric acid, phosphoric acid, serine, succinic acid, threonic acid and tyrosine have also been reported as distinguishing urinary metabolites and are reported as significant here.

Our findings for LPK rats are generally consistent with those published by Zhao *et al*. [21], who found that, among other differences, hippuric and uric acids were increased and arachidonic and docosahexaenoic acids were decreased in the kidney tissue of a CKD rat model. In their study, however, it was found that the purine nucleoside inosine was significantly decreased, while in our study it was significantly increased in LPK kidney

tissue. This difference may be due to the different models or alternatively/additionally the different stages and time frame of disease under study. Nonetheless, inosine and uric acid are related to purine metabolism, which has previously been identified as a potentially important pathway in PKD pathogenesis [14].

4.2 Liver tissue changes

There was no distinction between disease states for females based on liver metabolite profiles (Figure 5.3). This may be explained by the more rapid progression to ESRD in males than females as demonstrated by higher concentrations of serum urea and creatinine in males [24]. Interestingly, many of the significant metabolites found in this study were consistent (including pattern of fold change) with that observed by Kim *et al*. [42], who investigated fatty liver disease. This finding supports altered energy metabolism in the LPK rat. Pathways with three or more significant metabolites in the liver tissue included galactose metabolism, a previously reported pathway of interest [14], glutathione metabolism and glycine and serine metabolism, however these metabolites (glycine, cysteine, and glutamic acid) are common to each of the metabolic pathways listed. Interestingly, arachidonic acid, known to be involved in oxidative stress [43], and docosahexaenoic acid (alpha linolenic and linoleic acid metabolism), were significantly increased in liver tissue, but decreased in kidney tissue. Since there was no evidence for gross pathology in the liver of the LPK rats [24], these data suggest activated or dysfunctional signalling mechanisms of the hepatocytes which may result as a primary pathology due to the model used, or may be secondary to the kidney disease.

4.3 Limitations

The present study investigated the metabolic profiles of rat kidney and liver tissues from animals in whom kidney disease had progressed to a moderate stage. Significant biochemical changes were observed in both organs of diseased rats, revealing a metabolic phenotype of

PKD. Future investigations would be well served by the inclusion of sampling times correlating to other disease stages including earlier, before disease has had a significant impact on the animals, and later, as the animals progress to ESRD, potentially revealing metabolic signatures which change with disease progression. This would reveal informative diagnostic and prognostic markers beyond the biochemical changes revealed here. Further, with the inclusion of more numerous sampling and alternative quality control approaches [44] to feature acceptance, the interpretation of more subtle biochemical changes may be permitted and would complement the interpretation of these data. Added strength would come from the identification of as yet unidentified metabolites deemed significant in these data and is the subject of ongoing investigation.

5. Conclusion

We observed several significantly different metabolic phenotypes between the diseased LPK and Lewis control rat. These reported metabolites emphasise five pathways with three or more contributing metabolites in the kidney, and three biochemical pathways with three or more contributing metabolites in the liver. These metabolites have been shown to be diagnostically important in the urine, plasma and kidney tissue of other mouse and rat models of PKD and human PKD and CKD. Further, we demonstrate the ability of a metabolomics approach to ascertain biochemical change and associated pathways for further investigation.

Acknowledgements

The authors acknowledge Dr Ian Mullaney and Per Thomsen for their assistance with sample collection and Dr Stacey Reinke for her assistance with statistical analyses. Shimadzu Scientific Australasia are acknowledged for the GC-MS instrument.

Grants

The work described in this paper was supported by the NCRIS Metabolomics Australia and the School of Veterinary and Life Sciences, Murdoch University. Metabolomics Australia is a Bioplatforms Australia (BPA) funded initiative. H Abbiss was supported by an Australian Postgraduate Award. C Rawlinson and J P A Gummer were supported through BPA.

Disclosures

The authors declare that they have no conflict of interest.

References

[1] V.E. Torres, P.C. Harris, Y. Pirson, Autosomal dominant polycystic kidney disease, Lancet, 369 (2007) 1287-1301.

[2] P.C. Harris, V.E. Torres, Polycystic kidney disease, Annual Review of Medicine, 60 (2009) 321-337.

[3] K. Zerres, S. Rudnik-Schoneborn, C. Steinkamm, J. Becker, G. Mucher, Autosomal recessive polycystic kidney disease, J Mol Med, 76 (1998) 303-309.

[4] M.T. Wolf, Nephronophthisis and related syndromes, Curr Opin Pediatr, 27 (2015) 201-211.

[5] D.A. Braun, F. Hildebrandt, Ciliopathies, Cold Spring Harbor Perspectives in Biology, (2016).

[6] R.J. Simms, A.M. Haynes, L. Eley, J. Sayer, Nephronophthisis: a genetically diverse ciliopathy, International Journal of Nephrology, 2011 (2011) 1-10.

[7] S. Rossetti, P.C. Harris, Genotype-phenotype correlations in autosomal dominant and autosomal recessive polycystic kidney disease, Journal of the American Society of Nephrology, 18 (2007).

[8] H. Happé, E. de Heer, D.J.M. Peters, Polycystic kidney disease: The complexity of planar cell polarity and signaling during tissue regeneration and cyst formation, BBA-Mol Basis Dis, 1812 (2011) 1249-1255.

[9] V. Patel, R. Chowdhury, P. Igarashi, Advances in the pathogenesis and treatment of polycystic kidney disease, Curr Opin Nephrol Hy, 18 (2009) 99.

[10] W.E. Sweeney, E.D. Avner, Molecular and cellular pathophysiology of autosomal recessive polycystic kidney disease (ARPKD), Cell Tissue Res, 326 (2006) 671-685.

[11] Z.H. Bajwa, S. Gupta, C.A. Warfield, T.I. Steinman, Pain management in polycystic kidney disease, Kidney International, 60 (2001) 1631-1644.

[12] T. Toyohara, T. Suzuki, Y. Akiyama, D. Yoshihara, Y. Takeuchi, E. Mishima, K. Kikuchi, C. Suzuki, M. Tanemoto, S. Ito, S. Nagao, T. Soga, T. Abe, Metabolomic profiling of the autosomal dominant polycystic kidney disease rat model, Clinical and Experimental Nephrology, 15 (2011) 676-687.

[13] J. Boelaert, R. t'Kindt, E. Schepers, L. Jorge, G. Glorieux, N. Neirynck, F. Lynen, P. Sandra, R. Vanholder, K. Sandra, State-of-the-art non-targeted metabolomics in the study of chronic kidney disease, Metabolomics, 10 (2014) 425-442.

[14] S.L. Taylor, S. Ganti, N.O. Bukanov, A. Chapman, O. Fiehn, M. Osier, K. Kim, R.H. Weiss, A metabolomics approach using juvenile cystic mice to identify urinary biomarkers and altered pathways in polycystic kidney disease, American Journal of Physiology - Renal Physiology, 298 (2010) 909-922.

[15] H. Abbiss, G. Maker, J. Gummer, M.J. Sharman, J.K. Phillips, M. Boyce, R.D. Trengove, The development of a non-targeted metabolomics method to investigate urine in a rat model of polycystic kidney disease, Nephrology, 17 (2012) 104-110.

[16] A.D. Kistler, H. Mischak, D. Poster, M. Dakna, R.P. Wuthrich, A.L. Serra, Identification of a unique urinary biomarker profile in patients with autosomal dominant polycystic kidney disease, Kidney International, 76 (2009).

[17] S. Moreno, O. Ibraghimov-Beskrovnaya, N.O. Bukanov, Serum and urinary biomarker signatures for rapid preclinical in vivo assessment of CDK inhibition as a therapeutic approach for PKD, Cell Cycle, 7 (2008) 1856-1864.

[18] W. Gronwald, M.S. Klein, R. Zeltner, B.D. Schulze, S.W. Reinhold, M. Deutschmann, A.K. Immervoll, C.A. Boger, B. Banas, K.U. Eckardt, P.J. Oefner, Detection of autosomal dominant polycystic kidney disease by NMR spectroscopic fingerprinting of urine, Kidney International, 79 (2011) 1244-1253.

[19] L.F. Menezes, G.G. Germino, Systems biology of polycystic kidney disease: a critical review, WIREs Syst Biol Med, 7 (2015) 39-52.

[20] V.J. Hwang, J. Kim, A. Rand, C. Yang, S. Sturdivant, B. Hammock, P.D. Bell, L.M. Guay-Woodford, R.H. Weiss, The cpk model of recessive PKD shows glutamine dependence associated with the production of the oncometabolite 2-hydroxyglutarate, American Journal Of Physiology - Renal Physiology, 309 (2015) F492-F498.

[21] Y.-Y. Zhao, P. Lei, D.-Q. Chen, Y.-L. Feng, X. Bai, Renal metabolic profiling of early renal injury and renoprotective effects of *Poria cocos* epidermis using UPLC Q-TOF/HSMS/MS^{E}, Journal of Pharmaceutical and Biomedical Analysis, 81-82 (2013) 202-209.

[22] T.J. Velenosi, A. Hennop, D.A. Feere, A. Tieu, A.S. Kucey, P. Kyriacou, L.E. McCuaig, S.E. Nevison, M.A. Kerr, B.L. Urquhart, Untargeted plasma and tissue metabolomics in rats with chronic kidney disease given AST-120, Scientific Reports, 6 (2016) 22526.

[23] J.K. McCooke, R. Appels, R.A. Barrero, A. Ding, J.E. Ozimek-Kulik, M.I. Bellgard, G. Morahan, J.K. Phillips, A novel mutation causing nephronophthisis in the Lewis polycystic kidney rat localises to a conserved RCC1 domain in Nek8, BMC Genomics, 13 (2012) 1-16.

[24] J.K. Phillips, D. Hopwood, R.A. Loxley, K. Ghatora, J.D. Coombes, Y.S. Tan, J.L. Harrison, D.J. McKitrick, V. Holobotvskyy, L.F. Arnolda, G.K. Rangan, Temporal relationship between renal cyst development, hypertension and cardiac hypertrophy in a new rat model of autosomal recessive polycystic kidney disease, Kidney and Blood Pressure Research, 30 (2007) 129-144.

[25] K.G. Schwensen, J.S. Burgess, N.S. Graf, S.I. Alexander, D.C. Harris, J.K. Phillips, G.K. Rangan, Early cyst growth is associated with the increased nuclear expression of cyclin D1/Rb protein in an autosomal-recessive polycystic kidney disease rat model, Nephron Experimental Nephrology, 117 (2011) e93-e103.

[26] F. Hildebrandt, M. Attanasio, E. Otto, Nephronophthisis: disease mechanisms of a ciliopathy, Journal of the American Society of Nephrology, 20 (2009) 23-35.

[27] D. Chauveau, F. Fakhouri, J.P. Grunfeld, Liver involvement in autosomal-dominant polycystic kidney disease: therapeutic dilemma, Journal of the American Society of Nephrology, 11 (2000) 1767-1775.

[28] H. Abbiss, C. Rawlinson, G.L. Maker, R.D. Trengove, Assessment of automated trimethylsilyl derivatization protocols for GC-MS-based untargeted metabolomics analysis of urine, Metabolomics, 11 (2015) 1908-1921.

[29] J.P.A. Gummer, R.D. Trengove, R.P. Oliver, P.S. Solomon, Dissecting the role of G-protein signalling in primary metabolism in the wheat pathogen *Stagonospora nodorum*, Microbiology, 159 (2013) 1972-1985.

[30] Y. Benjamini, Y. Hochberg, Controlling the False Discovery Rate: A Practical and Powerful Approach to Multiple Testing, Journal of the Royal Statistical Society. Series B (Methodological), 57 (1995) 289-300.

[31] D.S. Wishart, T. Jewison, A.C. Guo, M. Wilson, C. Knox, Y. Liu, Y. Djoumbou, R. Mandal, F. Aziat, E. Dong, S. Bouatra, I. Sinelnikov, D. Arndt, J. Xia, P. Liu, F. Yallou, T. Bjorndahl, R. Perez-Pineiro, R. Eisner, F. Allen, V. Neveu, R. Greiner, A. Scalbert, HMDB 3.0--The Human Metabolome Database in 2013, Nucleic Acids Res, 41 (2013) D801-807.

[32] D.S. Wishart, C. Knox, A.C. Guo, R. Eisner, N. Young, B. Gautam, D.D. Hau, N. Psychogios, E. Dong, S. Bouatra, R. Mandal, I. Sinelnikov, J. Xia, L. Jia, J.A. Cruz, E. Lim, C.A. Sobsey, S. Shrivastava, P. Huang, P. Liu, L. Fang, J. Peng, R. Fradette, D. Cheng, D. Tzur, M. Clements, A. Lewis, A. De Souza, A. Zuniga, M. Dawe, Y. Xiong, D. Clive, R. Greiner, A. Nazyrova, R. Shaykhutdinov, L. Li, H.J. Vogel, I. Forsythe, HMDB: a knowledgebase for the human metabolome, Nucleic Acids Res, 37 (2009) D603-610.

[33] D.S. Wishart, D. Tzur, C. Knox, R. Eisner, A.C. Guo, N. Young, D. Cheng, K. Jewell, D. Arndt, S. Sawhney, C. Fung, L. Nikolai, M. Lewis, M.A. Coutouly, I. Forsythe, P. Tang, S. Shrivastava, K. Jeroncic, P. Stothard, G. Amegbey, D. Block, D.D. Hau, J. Wagner, J. Miniaci, M. Clements, M. Gebremedhin, N. Guo, Y. Zhang, G.E. Duggan, G.D. Macinnis, A.M. Weljie, R. Dowlatabadi, F. Bamforth, D. Clive, R. Greiner, L. Li, T. Marrie, B.D. Sykes, H.J. Vogel, L. Querengesser, HMDB: the Human Metabolome Database, Nucleic Acids Res, 35 (2007) D521-526.

[34] B.H. Junker, C. Klukas, F. Schreiber, VANTED: a system for advanced data analysis and visualization in the context of biological networks, BMC bioinformatics, 7 (2006) 109.

[35] W.B. Dunn, D. Broadhurst, P. Begley, E. Zelena, S. Francis-McIntyre, N. Anderson, M. Brown, J.D. Knowles, A. Halsall, J.N. Haselden, A.W. Nicholls, I.D. Wilson, D.B. Kell, R. Goodacre, Procedures for large-scale metabolic profiling of serum and plasma using gas chromatography and liquid chromatography coupled to mass spectrometry, Nat Protoc, 6 (2011) 1060-1083.

[36] E.M. Schwiebert, Compelling 'metabolomic' biomarkers may signal PKD pathogenesis, American Journal of Physiology - Renal Physiology, 298 (2010) F1103-F1104.

[37] A. Frolkis, C. Knox, E. Lim, T. Jewison, V. Law, D.D. Hau, P. Liu, B. Gautam, S. Ly, A.C. Guo, J. Xia, Y. Liang, S. Shrivastava, D.S. Wishart, SMPDB: The Small Molecule Pathway Database, Nucleic Acids Res, 38 (2010) D480-487.

[38] T. Jewison, Y. Su, F.M. Disfany, Y. Liang, C. Knox, A. Maciejewski, J. Poelzer, J. Huynh, Y. Zhou, D. Arndt, Y. Djoumbou, Y. Liu, L. Deng, A.C. Guo, B. Han, A. Pon, M. Wilson, S. Rafatnia, P. Liu, D.S. Wishart, SMPDB 2.0: big improvements to the small molecule pathway database, Nucleic Acids Res, 42 (2014) D478-484.

[39] H.G. Windmueller, A.E. Spaeth, Source and fate of circulating citrulline, American Journal of Physiology, 241 (1981) E473-480.

[40] J. Zhao, Plasma kynurenic acid/tryptophan ratio: a sensitive and reliable biomarker for the assessment of renal function, Renal failure, 35 (2013) 648-653.

[41] T. Kobayashi, Y. Matsumura, T. Ozawa, H. Yanai, A. Iwasawa, T. Kamachi, K. Fujiwara, N. Tanaka, M. Kohno, Exploration of novel predictive markers in rat plasma of the early stages of chronic renal failure, Analytical and Bioanalytical Chemistry, 406 (2014) 1365-1376.

[42] H.J. Kim, J.H. Kim, S. Noh, H.J. Hur, M.J. Sung, J.T. Hwang, J.H. Park, H.J. Yang, M.S. Kim, D.Y. Kwon, S.H. Yoon, Metabolomic analysis of livers and serum from high-fat diet induced obese mice, Journal of Proteome Research, 10 (2011) 722-731.

[43] M.A. Balboa, J. Balsinde, Oxidative stress and arachidonic acid mobilization, Biochimica et Biophysica Acta (BBA) - Molecular and Cell Biology of Lipids, 1761 (2006) 385-391.

[44] T. Sangster, H. Major, R. Plumb, A.J. Wilson, I.D. Wilson, A pragmatic and readily implemented quality control strategy for HPLC-MS and GC-MS-based metabonomic analysis, Analyst, 131 (2006) 1075-1078.

Figure headings

Fig. 1. 16-week old male Lewis (left) and LPK (right) rat left kidneys.

Fig. 2. Principal component analysis scores (A, C) and loadings (B, D) plots showing clear separation of LPK kidney tissue samples (■ LPK male; □ LPK female) from Lewis controls (● Lewis male; ○ Lewis female). Data were log-transformed (x = Log[x + 1]) and normalized to the sample weight (mg) (A, B); or the sample weight and the internal standard (C, D).

Fig. 3. Principal component analysis scores (A, C) and loadings (B, D) plots showing separation of male LPK liver tissue samples (■ LPK male; □ LPK female) from male Lewis controls (● Lewis male; ○ Lewis female). Data were log-transformed (x = Log[x + 1]) and normalized to the sample weight (mg) (A, B); or the sample weight and the internal standard (C, D).

Fig. 4. Schematic representation of the citric acid cycle showing metabolites which were decreased (blue), increased (orange) and unchanged (green) in the LPK kidney tissue samples (n=10) compared with the Lewis control (n=11). Although they did not meet the reporting criteria, 2-oxoglutaric acid and glutamic acid have been included. Glycine, cysteine, glutamic acid and urea were all increased in the LPK liver as well as the kidney.

Table 1. Whole animal, single kidney and total liver weight (g; mean ± SD) of Lewis and LPK rats, measured at 16 weeks of age. Data represent the combined male and female measurements (Lewis n = 11; LPK n = 10).

	Lew	LPK	p-value
Body weight (g)	336.45 ± 94.96	220.48 ± 46.78	0.003
Kidney weight (frozen wet; g)	1.29 ± 0.34	7.78 ± 2.21	<0.001
Kidney weight (dry; g)	0.40 ± 0.15	0.59 ± 0.14	0.008
Liver weight (frozen wet; g)	10.78 ± 3.30	5.73 ± 0.91	<0.001
Liver weight (frozen wet; g), % BW	3.19 ± 0.26	2.64 ± 0.29	<0.001
Liver weight (dry; g)	3.19 ± 1.03	1.65 ± 0.28	<0.001
Liver weight (dry; g), % BW	0.94 ± 0.09	0.76 ± 0.06	<0.001

Table 2. Number of features (mean ± SD) in Lewis and LPK rat kidney and liver tissue samples and summary of the number of identified metabolites and significant features/metabolites detected in the kidney and liver tissue of Lewis and LPK rats.

	Kidney		Liver	
	$^{(11)}$Lew	$^{(10)}$LPK	$^{(11)}$Lew	$^{(8)}$LPK
Number of features	325 ± 26	623 ± 51	269 ± 14	281 ± 13
Number of features in 100% replicates of one strain only	12	73	0	0
Number of features in > 80% of replicates*	146		167	
Number of identified metabolites	109		64	
Number of significant features ($p < 0.05$)	122		30	
Number of identified significant metabolites	51		18	
Number of unique identified significant metabolites	47		14	

* $n > 17$ out of $n = 21$ individuals tested

Highlights

- There were marked differences in metabolites of the kidney tissue with 122 metabolites significantly different between the LPK and Lewis strains
- There were 30 metabolites which were significantly different between strains for liver samples
- Five biochemical pathways showed three or more significantly altered metabolites

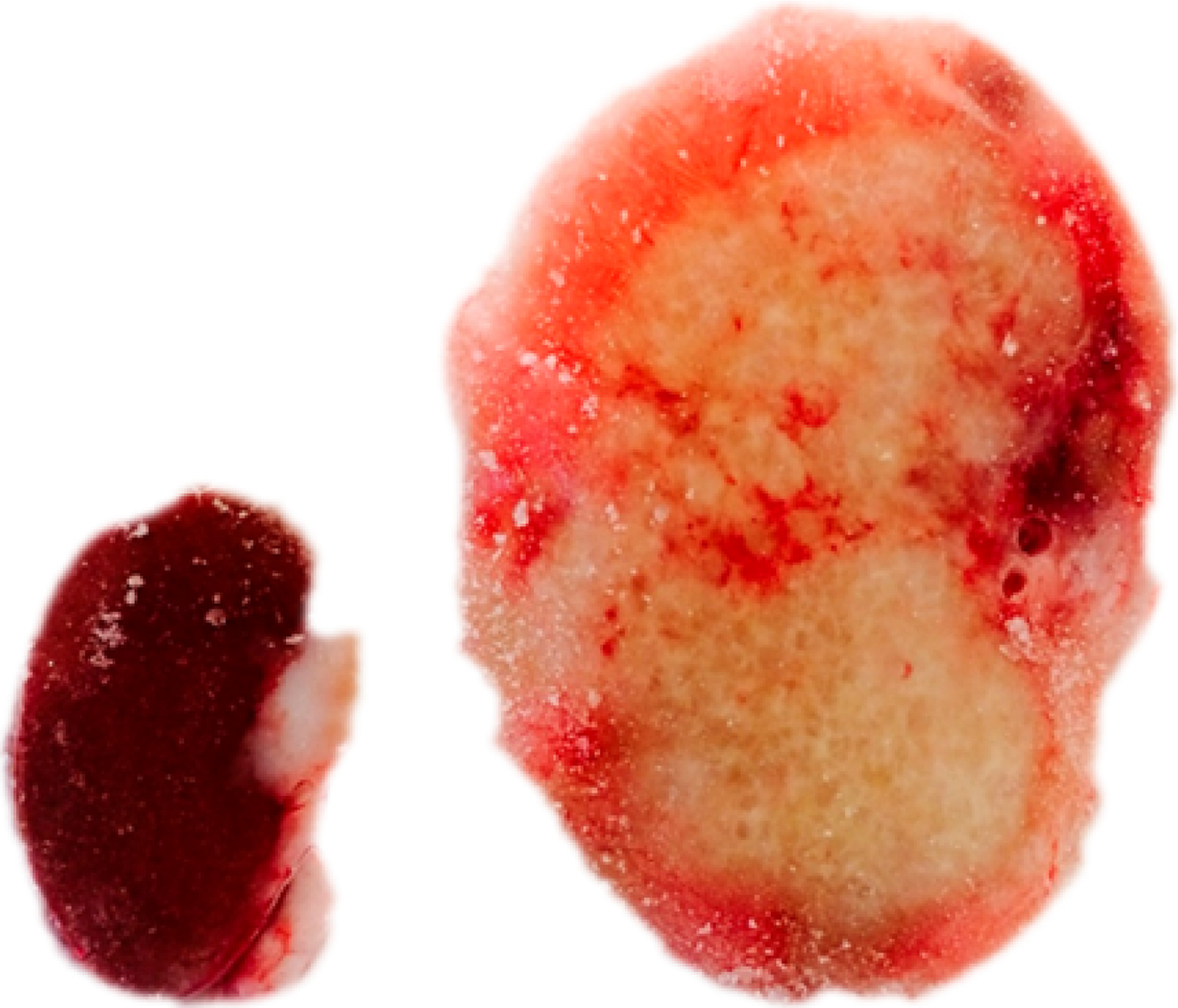

Figure 1

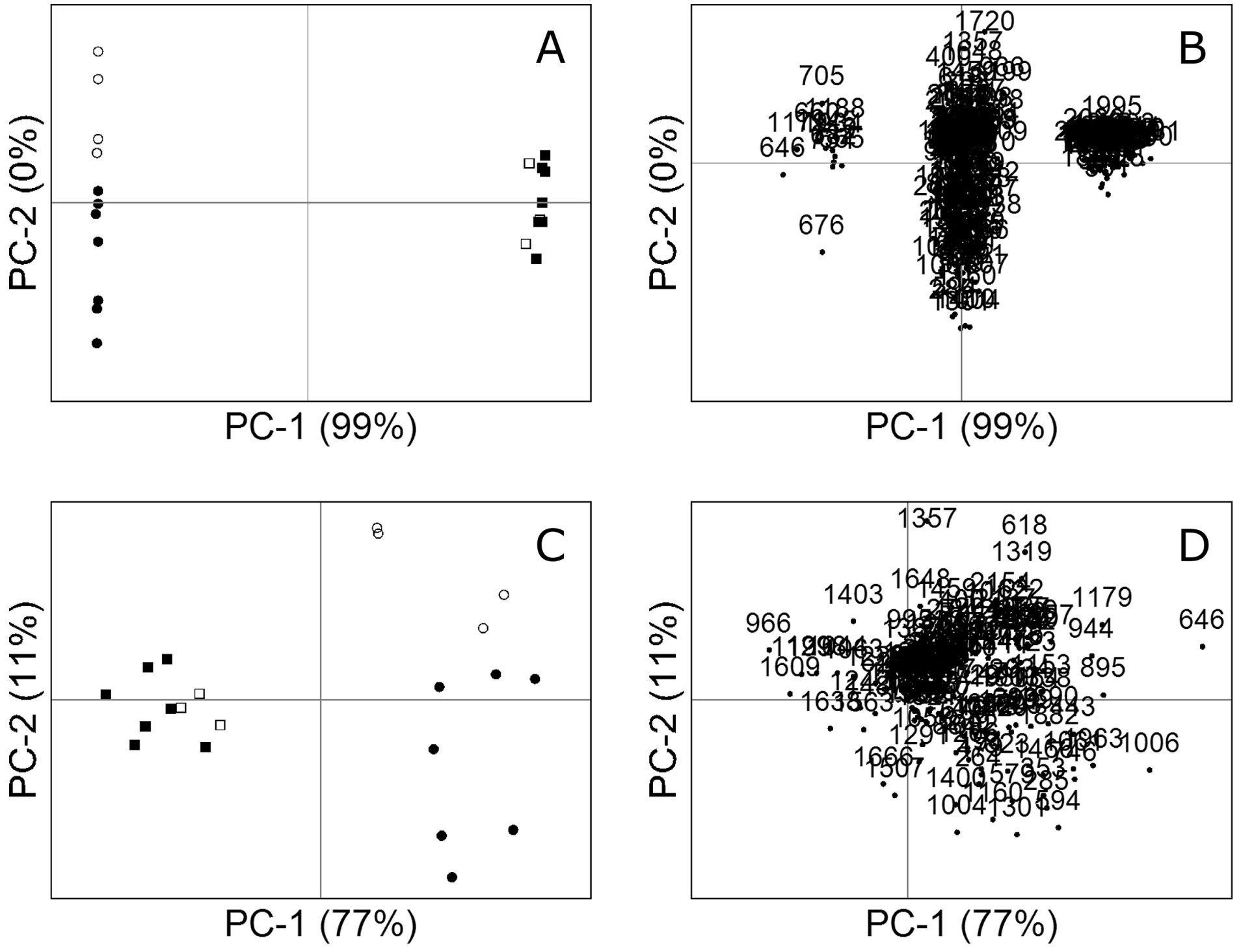
A
PC-2 (0%)
PC-1 (99%)
B
PC-2 (0%)
PC-1 (99%)
705
646
676
1720
1995
C
PC-2 (11%)
PC-1 (77%)
D
PC-2 (11%)
PC-1 (77%)
1357
618
1319
1403
1179
966
646
944
1609
895
1006

Figure 2

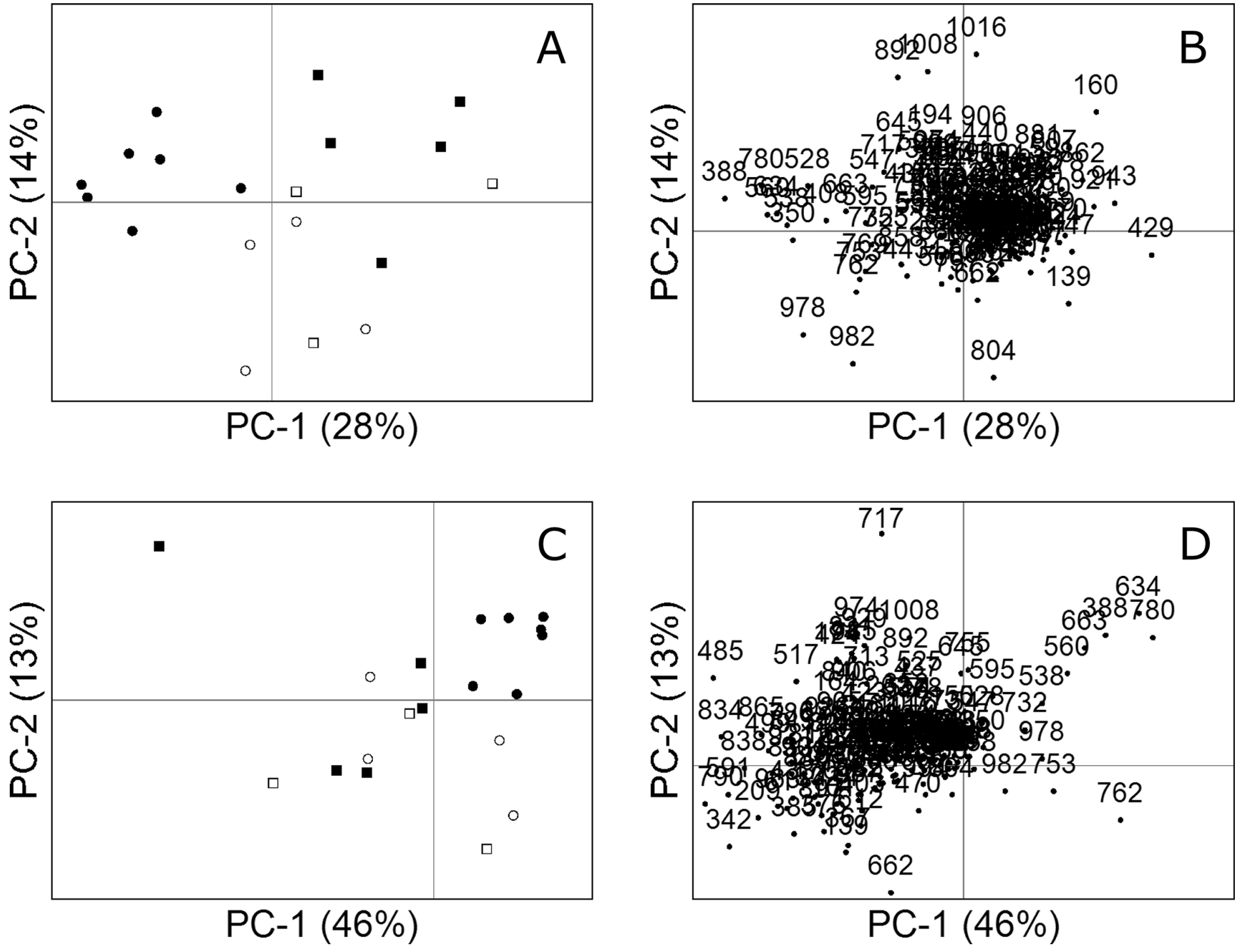

Figure 3

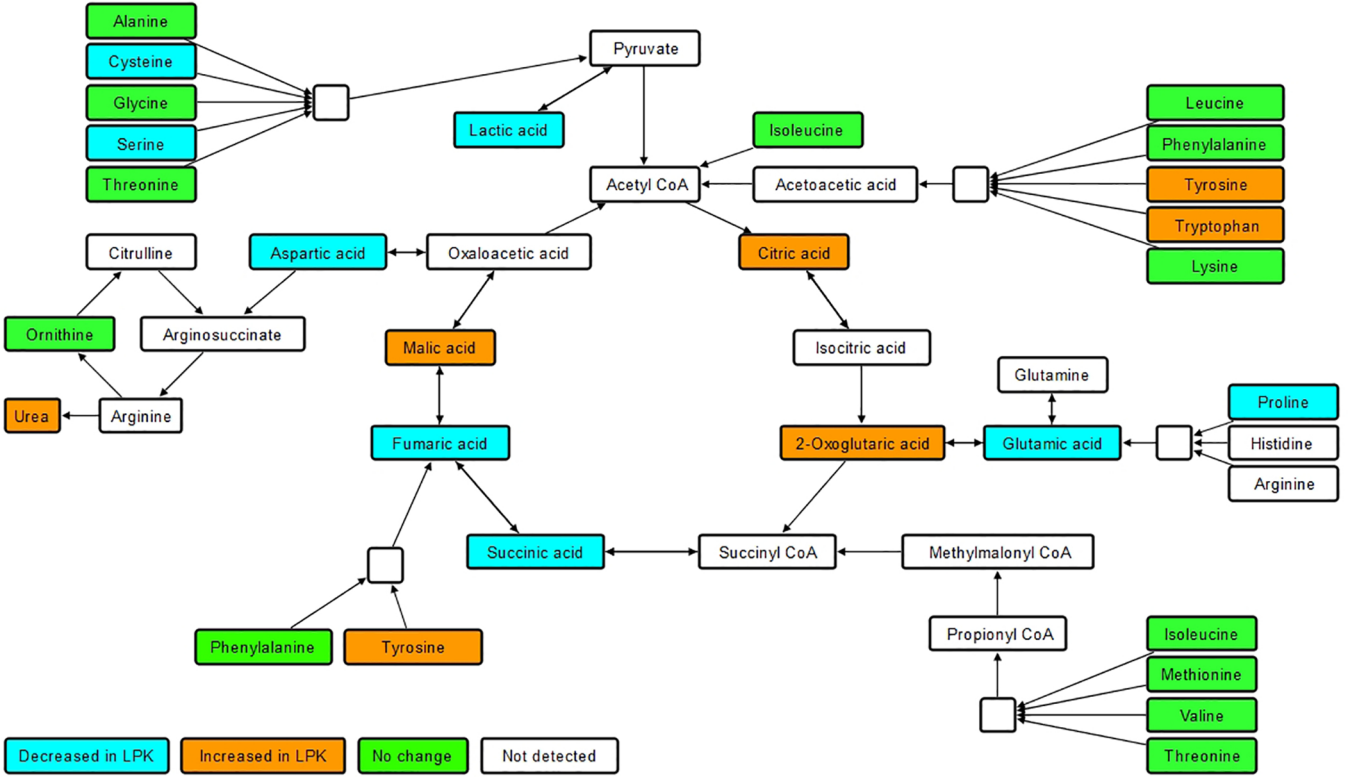
Alanine
Cysteine
Glycine
Serine
Threonine
Pyruvate
Lactic acid
Isoleucine
Leucine
Phenylalanine
Tyrosine
Tryptophan
Lysine
Acetyl CoA
Acetoacetic acid
Citrulline
Aspartic acid
Oxaloacetic acid
Citric acid
Ornithine
Arginosuccinate
Malic acid
Isocitric acid
Glutamine
Urea
Arginine
Proline
Histidine
Arginine
Fumaric acid
2-Oxoglutaric acid
Glutamic acid
Succinic acid
Succinyl CoA
Methylmalonyl CoA
Phenylalanine
Tyrosine
Propionyl CoA
Isoleucine
Methionine
Valine
Threonine
Decreased in LPK
Increased in LPK
No change
Not detected

Figure 4